CHINESE JOURNAL OF GEOPHYSICS Vol.59, No.5, 2016, pp: 474–487

INFLUENCES OF THERMAL FORCING OVER THE SLOPE/PLATFORM OF THE TIBETAN PLATEAU ON ASIAN SUMMER MONSOON: NUMERICAL STUDIES WITH THE WRF MODEL

WANG Zi-Qian[1,2], DUAN An-Min[2], LI Mao-Shan[3], HE Bian[2]

1 *School of Atmospheric Sciences, Sun Yat-sen University, Guangzhou* 510275*, China*

2 *State Key Laboratory of Numerical Modeling for Atmospheric Sciences and Geophysical Fluid Dynamics, Institute of Atmospheric Physics, Chinese Academy of Sciences, Beijing* 100029*, China*

3 *Key Laboratory for Land Surface Process and Climate Change in Cold and Arid Regions, Chinese Academy of Sciences, Lanzhou* 730000*, China*

Abstract With the global warming, the evolution of Asian summer monsoon (ASM) becomes more complicated, while the thermal effect of the Tibetan Plateau (TP) is an important forcing to the variability of weather and climate in ASM region. Regional climate model (RCM) is a useful tool in the regional climate change research and has higher resolutions that can represent topography and land surface processes more accurately comparing with atmospheric general circulation models (AGCMs). In this study, the impact of thermal forcing over different terrains of TP on ASM (including South and East ASM (SASM and EASM)) is investigated using the Weather Research and Forecasting (WRF) model. Results indicate that the local circulation and precipitation around the Himalayas (HIM) are significantly influenced by the surface heating over the HIM's southern slope, which is a dominant factor for the formation of the north branch of SASM. Meanwhile, the climbing moist airflow and precipitation over the southern slope of TP are mainly induced by HIM's thermal forcing. Due to HIM's sloping heating, the upper-level troposphere warm center is steadily located over the HIM area and the EASM is also intensified obviously (Characterized both by the enhanced low-level southwesterly over East China and the enhanced southward anomalous dry-cold northerly). As to the surface heating over TP's platform region (PL), although its influence on the summer monsoon circulation and precipitation is weaker than the HIM's, it induces a wider response of SASM and a stronger influence on the meridional Hadley circulation. The PL's heating is able to regulate low-level southwesterly over the remote tropical ocean. Furthermore, a comparison of multiple monsoon indices reveals that both HIM sloping heating and PL heating can intensify SASM or EASM, but the impacts of thermal forcing over different terrains are distinct on the two subsystems of ASM.

Key words Tibetan Plateau; Thermal forcing; Asian summer monsoon; WRF model

1 INTRODUCTION

Both the South and East Asian summer monsoon (SASM and EASM) are the distinctive subsystems of Asian summer monsoon (ASM). The ASM is the most representative monsoon system in the world, and its abnormal activities directly affect the weather and climate of South and East Asian countries. Under the background of global warming, the variations of ASM become more and more complicated (Webster, 2006), meanwhile extreme events occurred frequently over the monsoon region (Herring et al., 2014). Human beings suffer great economic losses from flood, drought, or extreme high temperature induced by the abnormal summer monsoon. Thus, the formation, maintenance and variation of ASM are widely concerned by scientists in a long time.

Previous studies have indicated that the precipitation and circulation of ASM is closely connected with the mechanical or thermal forcing of the Tibetan Plateau (TP) (e.g. Flohn, 1957; Ye et al., 1979; Wu and Zhang, 1998; Zhao and Chen, 2001; Li, 2003; Liang et al., 2006; Yu and Hu, 2008; Xu et al., 2010; Wang et al., 2014b). In spring and summer, surface sensible heating is strong over the TP, and the thermal forcing exerts

E-mail: wangziq5@mail.sysu.edu.cn

a great impact on ASM (e.g. Wu et al., 1997; Mao and Wu, 2006; Wu et al., 2007; He et al., 2011). However, some recent studies (Boos and Kuang, 2010, 2013; Molnar et al., 2010) argued that the TP thermal forcing is not the dominant driving force influencing ASM. Boos and Kuang (2010) removed the terrain over the main TP, while Himalayas (HIM) was only reserved in the Community Atmosphere Model (CAM) and Community Earth System Model (CESM), and the simulated result of ASM was much similar as that in the whole terrain experiment. Then they claimed that the dominant factor for the formation and maintenance of ASM is the mechanical effect of HIM, but not the thermal forcing. However, Wu et al. (2012) insisted that TP's thermal forcing plays a dominant role in the formation of ASM by using the Spectral Atmospheric Model of Institute of Atmospheric Physics (SAMIL). They pointed out that sensible heating over the southern slope of TP was still retained in the experiment of Boos and Kuang (2010), thus air-pumping effect due to the sensible heating was still existed. Then it cannot deny the dominant effect of the TP's thermal forcing in affecting ASM. When the surface heating over the southern slope of the TP was also simultaneously suppressed, it was shown that the northern branch of SASM disappeared (Wu et al., 2012).

From the above review, whether the TP's thermal or mechanical forcing is dominant in the formation and maintenance of SASM is still controversial. Meanwhile, previous studies have shown that numerical model can depict the SASM very well even though only the terrain of HIM is kept in the model, implying that the impacts of thermal forcing over different areas of the TP on SASM or other ASM subsystem (such as EASM) are different. The surface heating over the southern slope of the TP has a significant impact on SASM, but how is the thermal effect of the TP's platform (PL)? Which part of the TP (HIM or PL) is more important? There is less attention focusing on these fields so far. Besides the influence on SASM, the effects of orographic heating over the different areas of TP on EASM also need further investigation. In addition, when discussing the thermal forcing over the HIM and PL on SASM, all previous numerical studies were based on global climate system models, which had a coarse grid about 180∼200 km. And the coarse model may lead to extra uncertainty, especially over and around the TP with complicated orography. Therefore, this study will apply a high resolution regional model (WRF, Weather Research and Forecasting) to further understand the thermal forcing of TP on the ASM. We will try to reveal the differences of the thermal forcing over TP's different area on the atmospheric circulation and precipitation.

2 MODEL AND EXPERIMENTAL DESIGN

The WRF model version 3.4.1 (Skamarock et al., 2008) is used in this study. With the continuous development and improvement, WRF model has been employed previously as a RCM to simulate the variations of summer monsoon (e.g. Kim and Hong, 2010; Yu et al., 2011; Yang et al., 2012; Wang et al., 2014a). Compared with atmospheric general circulation models, the WRF has a higher resolution that represents meso- and small-scale dynamic and physical processes more accurately. It is a useful tool in the study of weather and climate over the TP and its surrounding areas with complex topography. The physical packages of WRF used in this study include the WRF Single-Moment 6-Class (WSM6) microphysics scheme, the Grell-Devenyi (GD) convective scheme, the Noah land surface model, the BouLac planetary boundary layer (PBL) scheme, the Goddard shortwave scheme, and the Rapid Radiative Transfer Model (RRTM) for long wave radiation. The spatial domain of simulations covers most of Asia and the adjacent oceans with 133 grid points latitudinally and 195 grid points longitudinally (a buffer zone had five grid points). A Lambert projection is adopted and the domain is centered at 30°N, 95°E (Fig. 1). The model has a 45 km horizontal resolution and 35 vertical layers with a prescribed model top at 50 hPa. The initial state of the atmosphere and lateral boundary conditions (updated every 6 hours) are obtained from the Final Analysis of National Centers for Environmental Prediction (NCEP-FNL, http://rda.ucar.edu/datasets/ds083.2/), and sea surface temperature (SST) forcing data set is the Optimum Interpolation SST from National Oceanic and Atmospheric Administration (NOAA), which is updated daily. We also used Tropical Rainfall Measuring Mission (TRMM) 3B42 daily rainfall data to verify the simulated results of monsoon precipitation.

In the associated previous studies, the division of HIM and PL in each experiment was achieved by asplit line that was defined as the two-thirds of maximum elevation at each particular longitude (Boos and Kuang, 2010; Wu et al., 2012). Or the boundary line was directly considered to be the elevation of 4 km, namely the south of 4 km elevation is HIM and the north is PL (He, 2012). While in the higher-resolution WRF model, both previous definitions of the north-south boundary line are lower than the maximum elevation of the HIM. As a result, it is necessary to redefine the division of HIM and PL areas. Here, the TP's southern slope (HIM) is designed as the area between 70°E and 105°E where topography is above 300 m and below the maximum elevations at each longitude. If the maximum elevation was located within the central TP to the north of the Himalayas, then the next maximum elevation to its south was chosen (such as 92°E in Fig. 2a). Then the north of HIM is called PL shown as the white dotted region in Fig. 2b.

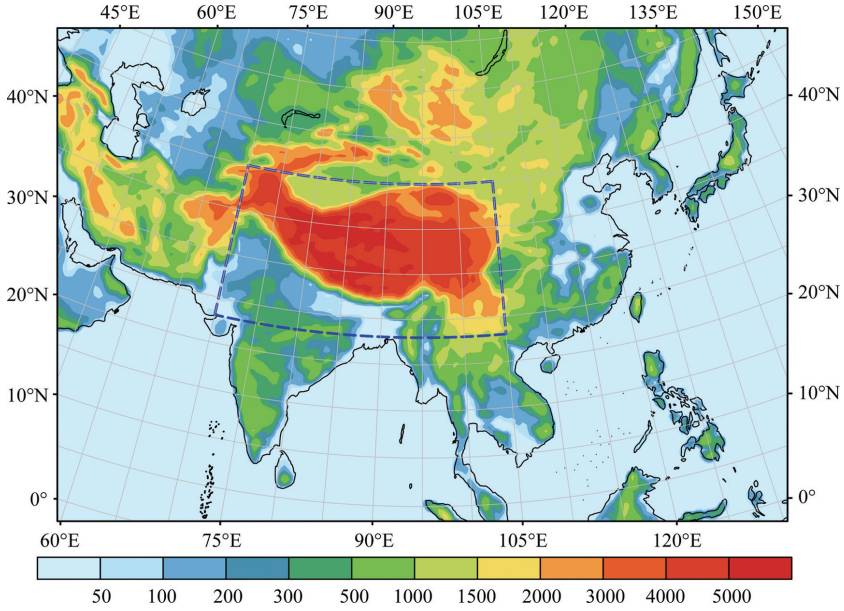

Fig. 1 WRF model domain and terrain height (shading, unit: m)
Dashed box is the area for sensitivity experiment over the Tibetan Plateau (TP).

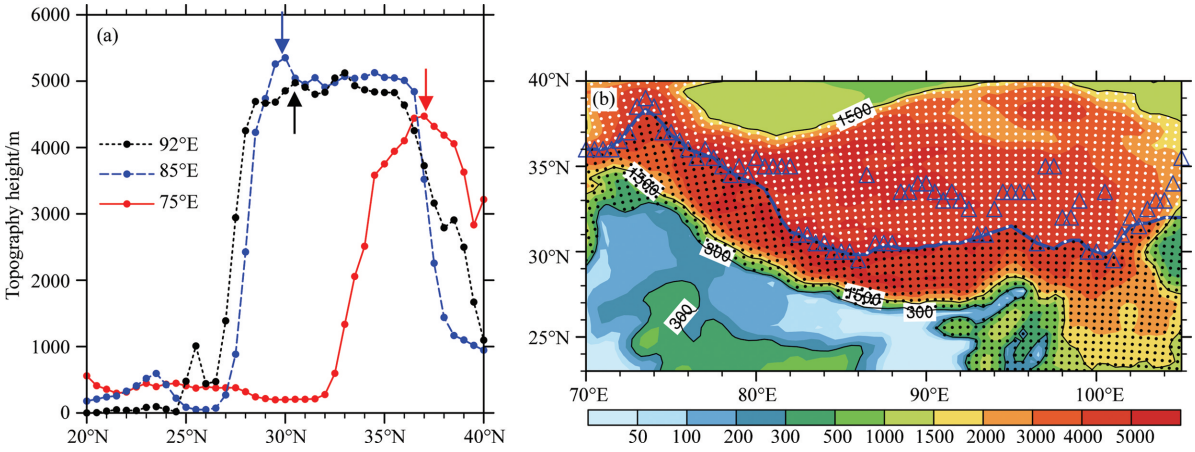

Fig. 2 (a) Topography height at different longitude. Arrows present the north boundary of the Himalayas' (HIM); (b) Terrain height (unit: m) over the sensitivity experiment area (23°N–40°N, 70°E–105°E). Blue triangles denote the highest point along every longitude, and the blue curve presents the boundary between HIM and TP's platform. The area over the south of blue curve and with topography above 300 m denotes the southern slope of HIM (black dotted region), and the area over the north of blue curve and with topography above 1500 m denotes the TP's platform (white dotted region)

Four ensemble experiments were performed and each incorporated six summers (2003–2008) with the initial conditions set at 0000 UTC May 1. The integration time was 4 months, i.e., every experiment ended at 1800 UTC August 31, and the output data derived from the final 3 months (June-August, JJA) were analyzed. Table 1 shows the details of the experimental design. The normal experiment with the WRF model was named the control run (CTL). One sensitive experiment (HIM_NS) was used to remove the surface sensible heating over the southern slope of the TP. To illustrate the thermal effect over the PL area, surface heating of the platform is suppressed in PL_NS. Besides, the third sensitive run (TP_NS) removed the surface heating over the whole

Table 1 Detail of experimental design

Experiments	Thermal forcing over the TP (Sensible heating)	
	Himalayas' sloping heating (HIM)	TP's platform heating (PL)
CTL	Yes	Yes
HIM_NS	No	Yes
PL_NS	Yes	No
TP_NS	No	No

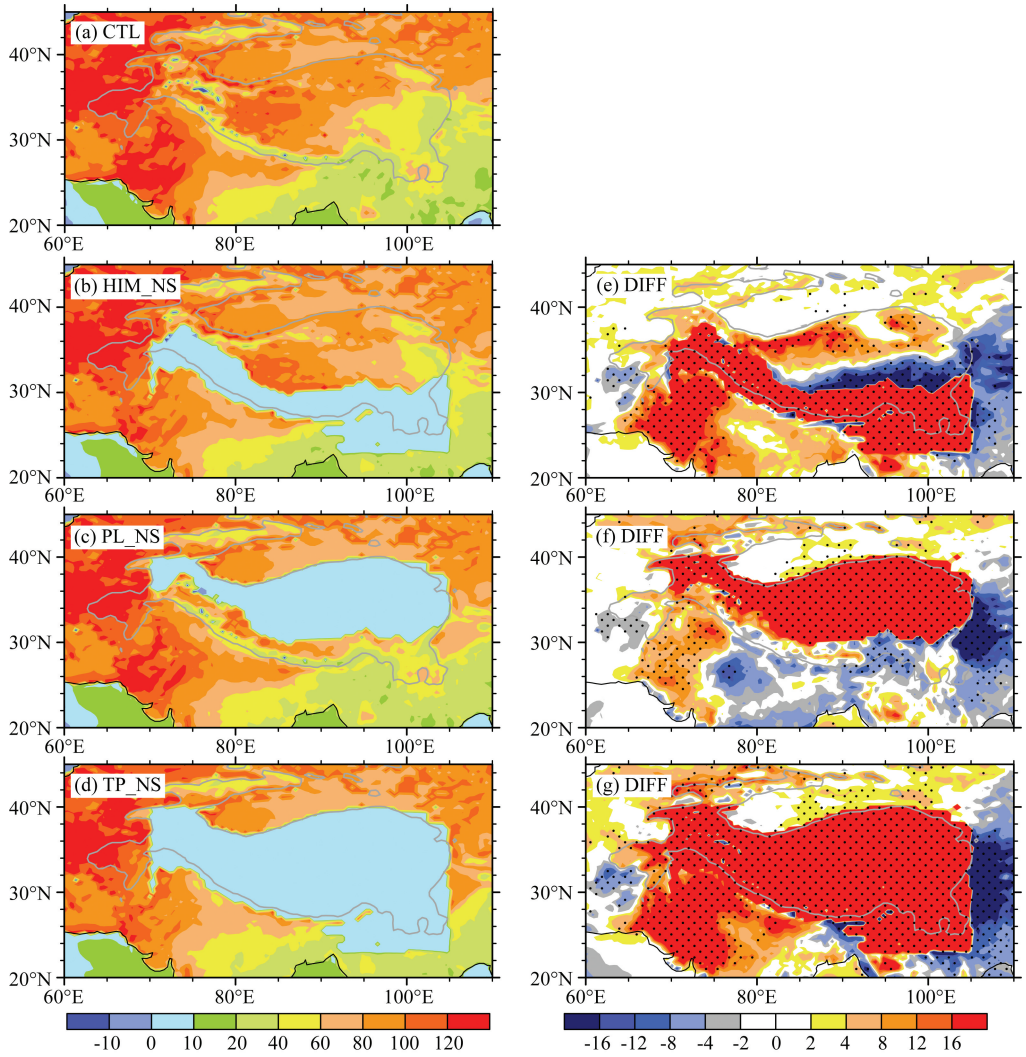

Fig. 3 Summer mean surface sensible heating (unit: $W \cdot m^{-2}$) for experiments of (a) CTL, (b) HIM_NS, (c) PL_NS, and (d) TP_NS; (e) CTL minus HIM_NS; (f) CTL minus PL_NS; (g) CTL minus TP_NS

Dotted regions in (e-g) denote the statistical significance of differences above 95% level.

TP area. Method of removing the thermal forcing was achieved by setting the surface sensible heating released into the atmosphere to zero at each time-step and each grid over the experimental region, while land surface energy balance was maintained. As such, SH is still computed by the land model at each time-step and allowed to influence land surface temperature. Figs. 3(a-d) show the spatial distributions of the JJA average surface sensible heating over the TP and its surrounding areas. The maximum surface heating is located over the northwestern TP in summer (>100 $\mathrm{W\cdot m^{-2}}$). In contrast, surface heating is weakest (<40 $\mathrm{W\cdot m^{-2}}$) over the southeastern TP due to the impact of summer monsoon rainfall.

3 RESULTS

3.1 Responses of the Monsoon Circulation, Precipitation, and Air Temperature

Figure 4 shows the summer mean precipitation and 850 hPa wind field from observations and WRF simulations. Comparing CTL (Fig. 4a) with observations (Fig. 4e), we find that WRF model can simulate summer precipitation and circulation very well and better than the coarse global climate models (Boos and Kuang, 2010; Wu et al., 2012) over low-latitude tropical oceans and East Asia. Especially in the TP region, WRF model can depict the large precipitation center successfully over the southern TP and also the gradual retreat characteristic of precipitation from southeast to northwest of the whole TP. These results make the sensitive experiments more reliable. Thermal forcing in different areas of the TP has different impacts on ASM (Figs. 4(f-h)). Differences between control experiment (CTL) and HIM_NS indicate that Himalayas' sloping heating has a significant impact on surrounding circulations. Thermal forcing of HIM enhances dry-cold air from high latitude over the western TP and the convergence of wet-warm airflow to the southern TP. Moreover, enhanced surface sensible heating appeared over the northwestern India and Pakistan due to the abnormal dry-cold air from high latitudes (Fig. 3e), which leads to a stronger cyclonic circulation over the southwestern TP. Meanwhile, the abnormal dry-cold airflow also suppresses summer precipitation over northwestern India and Pakistan (Fig. 4f). In addition, thermal forcing of HIM benefits the climbing and convergence of warm-wet airflow to the southern TP. And such effect produces more summer precipitation over that area. Once surface heating of HIM is suppressed, there is almost no precipitation over the southern TP (Fig. 4b). As regarding the response of EASM, heating of HIM enhances both the low-level southwest monsoon flow and the abnormal cold-dry air from northern high latitudes over East China. The convergence of southern and northern airflows leads to increased summer precipitation over East China (Fig. 4f). The cold-dry northerly anomalies over North China are induced by an upper-level Roosby wave train stimulated from the TP's heating (Wang et al., 2014b). With the equivalent barotropic structure, the low-level northerly is corresponding with the northwesterly at the west of the upper-level abnormal cyclonic circulation (Fig. 6e), which brings cold-dry airflow over North China.

Based on the global climate model, the thermal effect of TP's platform (PL) has been testified that it has limited impact on 850 hPa wind field and plays a weak role in controlling the SASM (He, 2012). From our sensitive experiment (PL_NS) with WRF model, both the responses of circulation and precipitation of SASM are truly weaker than those in HIM_NS. But the PL's heating has a wider influence on SASM, Fig. 4g shows that the tropical southwesterly is enhanced significantly over the Arabian Sea (AS) and the Bay of Bengal (BOB). The incidental enhanced moisture transport is beneficial for more precipitation over the northern BOB, Indian continent, and the west coast of India. When the surface heating over platform is removed, local precipitation is also suppressed. The PL's heating is conducive to the northward boost of southwest monsoon circulation over East Asia and the enhancement of monsoon precipitation in East China, which is similar to the heating effect of HIM. But the PL's heating exerts little influence on the cold-dry airflow from high latitudes over North China, thus the difference of precipitation over East China is less significant compared with that in HIM_NS. In addition, when the heating over the whole TP is removed (Fig. 4h), the response is presumably the composite effect of HIM's heating and PL's heating. The huge orographic heating significantly enhances the cold-dry flow around the western TP, the convergence of tropical southwest monsoon flow to the southern TP, and the northward boost of EASM over East China. Such circulations induce the enhancement of sensible heating and

weakening of precipitation over northwestern India and Pakistan (Fig. 3g), while the precipitations over the TP and East China are increased.

From the above simulated results, we find that sensible heating of the TP is the primary cause for the occurrences of local precipitation. Once surface heating is removed, precipitation over the southern slope or platform of the TP disappeared. There is slight precipitation occurring over the southern slope of the TP even though the heating is suppressed (Fig. 4b and Fig. 4d), our previous study (Wang et al., 2015) explained that it

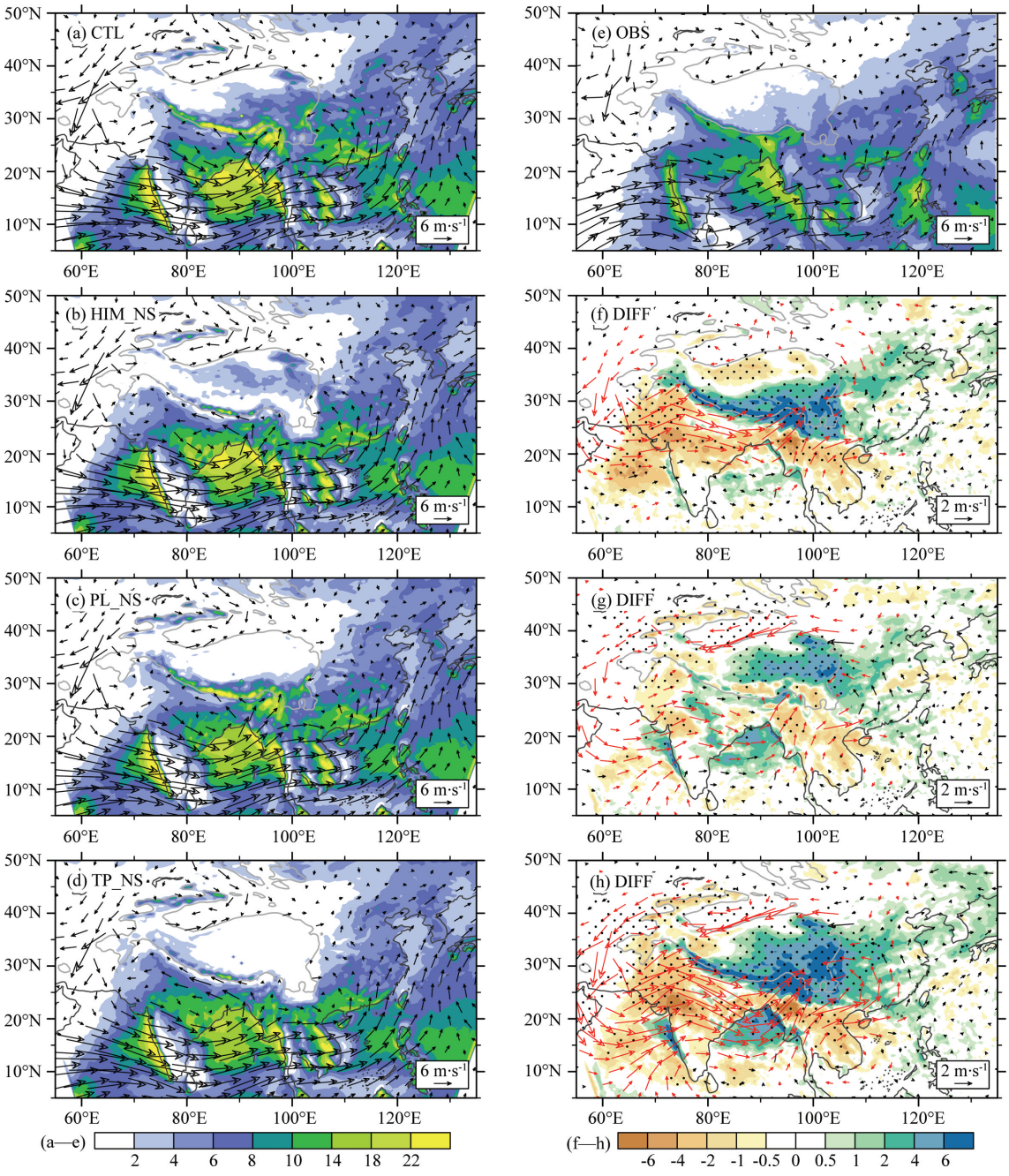

Fig. 4 Summer mean precipitation (shading, unit: mm·day^{-1}) and wind field at 850 hPa (vectors, unit: m·s^{-1}) for experiments of (a) CTL, (b) HIM_NS, (c) PL_NS, (d) TP_NS, and (e) OBS (wind is from NCEP-FNL, precipitation is from TRMM), (f) CTL minus HIM_NS, (g) CTL minus PL_NS, (h) CTL minus TP_NS

Dotted regions denote the statistical significance of precipitation anomalies above 95% level, and wind differences significant above 95% level are plotted in red color in (f-h).

is just owing to microphysical phase change of moisture. Fig. 5 gives the near-surface (σ=0.98) circulation over the TP and its surrounding area. And the near-surface wind field is further decomposed into flow around (encircling) and flow over (climbing) the TP based on the method of Qian et al. (1988) and Zhang and Qian (1999). In climatology, a cyclonic circulation always exists over the TP surface (Fig. 5b), and there is obvious climbing airflow over the southern and eastern slope. Especially over the southern slope of the TP, warm-wet airflow from tropical oceans climbs and uplifts, and then converges to lead to rainfall. When the Himalayas' sensible heating is removed, the climbing airflow over the southern slope is weakened (Fig. 5d), and the northward warm-wet airflow from BOB turns to encircling flow around the steep slope. The airflow around the southern slope of TP is obviously stronger than that in CTL experiment (Fig. 5a and Fig. 5c). Thus, the tropical warm-wet airflow cannot be uplifted over the southern slope of the TP if the local heating is removed, and then local precipitation is also suppressed. On the other hand, if only the PL's surface heating is removed

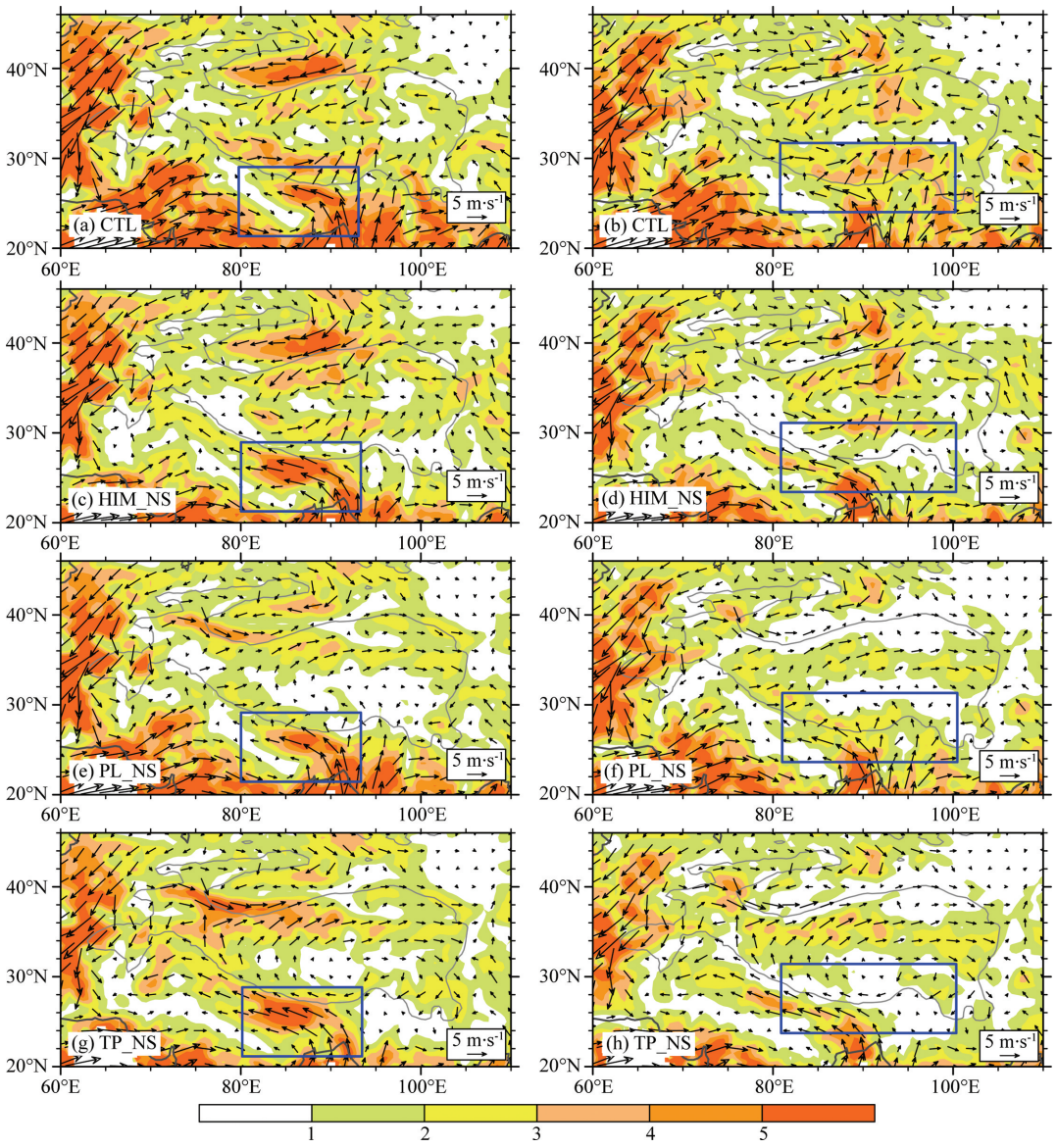

Fig. 5 Summer means of surface (σ = 0.98) wind (vectors), intensity of encircling flow (shading at left column), and intensity of climbing flow (shading at right column) for the experiments of (a-b) CTL, (c-d) HIM_NS, (e-f) PL_NS, and (g-h) TP_NS (unit: m·s^{-1})

Blue boxes represent the critical regions of encircling flow and climbing flow over the southern slope of TP.

but the HIM' heating remains, an anti-cyclonic circulation occurs near the surface of TP (Fig. 5f). It is indicated that the surface cyclone in summer is mainly modulated by the platform heating. While the climbing airflow still exists over the southern TP, which is beneficial for maintenance of precipitation over the slope. But the intensity of climbing airflow becomes weaker. Meanwhile, the absence of PL's heating suppresses the climbing airflow over the eastern slope of TP, which directly cuts off the moisture transport from the east boundary. Finally, if the heating over the whole TP is removed, TP is totally controlled by a near-surface anticyclone. Climbing airflow disappears absolutely surrounding the TP, and moisture transport to the TP is also suppressed. While the flow around the southern slope is enhanced, similar to the result obtained from HIM_NS (Fig. 5g and Fig. 5h).

Due to the high altitude, surface heating of the TP can directly or indirectly influence the upper-middle troposphere. Thus, TP's thermal forcing not only has a great impact on low-level monsoon circulation and precipitation, but also plays a role in the changes of upper-level circulation and temperature structures. In the CTL experiment, a huge anticyclonic circulation (i.e. South Asian High) appears over the upper-level TP in summer whose center locates over the southern slope of the TP, which is corresponding to a warm core (Fig. 6a). Such warm core weakens significantly and moves to northern India when the HIM's heating is removed (Fig. 6b). It is indicated that the heating over the southern slope of TP plays an important role in warming upper-level troposphere and locating the warm core over the slope. The difference between CTL and HIM_NS (Fig. 6e) also shows that HIM's heating mainly occur over the southern slope and enhances the South Asian High. At the meantime, the heating center stimulates an abnormal cyclone over the northeastward downstream area, which is similar to the previous results that TP's heating can motivate a large scale wave activity and downstream transport (Wang et al., 2008a; Wang et al., 2014b). The PL's heating has a wider and stronger impact on the upper-level circulation, covering the whole TP area. Due to the maximum sensible heating occurs over the northwestern TP in summer (Figs. 3a and 3b), the abnormal anticyclone locates over the western TP. Because of its wider and stronger influences, PL's heating has a larger scale possible impact on the land-sea thermal contrast and the meridional circulation. For example, former result (Fig. 3g) has shown that it can influence the remote southwest monsoon over the tropical ocean. In addition, the upper-level warm core cools more than 4 K if the whole TP heating is removed, and the South Asian High weakens greatly (Fig. 6d and Fig. 6g).

3.2 Vertical Structure of Monsoon

The thermal forcing in different areas of the TP has a diverse impact on upper-level troposphere temperature, and the incidental variational meridional temperature gradient may influence the vertical structure of monsoon. Fig. 7 shows the vertical circulation averaged from 85°E to 90°E for the four experiments. In CTL experiment, the SASM has two ascending airflows, i.e. the southern branch around 20°N and the northern branch over the Himalayas' slope. In addition, there is another ascending airflow over the northern slope of the TP, but it is much weaker than the northern branch of the SASM. That is because the ascending airflow over the northern slope of TP mainly originates from high latitudes (cold-dry airflow) and the associated condensational heat released from precipitation is rather weak. The positive feedback between condensational heat and ascending motion over the northern TP is less significant. Fig. 7b is the result of suppressed surface heating over HIM, and the northern branch of SASM disappeared, which is similar to the result from Wu et al. (2012). It is revealed that the HIM's heating plays a dominant role in the formation and maintenance of the northern branch of SASM. While the land-sea thermal contrast primarily controls the southern branch of SASM (Wu et al., 2012). But it is easy to find that the southern branch of SASM in HIM_NS is much wider than that in the CTL. After removing the HIM's heating, the southward cold-dry airflow from high latitudes over the western TP is weakened significantly (Fig. 4f), which is beneficial for the northward movement of the tropical warm-wet airflow. As a result, the southern branch of SASM expands northward. It is noted that summer precipitation over the central India (20°N-25°N) is increased in the experiment of HIM_NS. But it cannot be concluded that

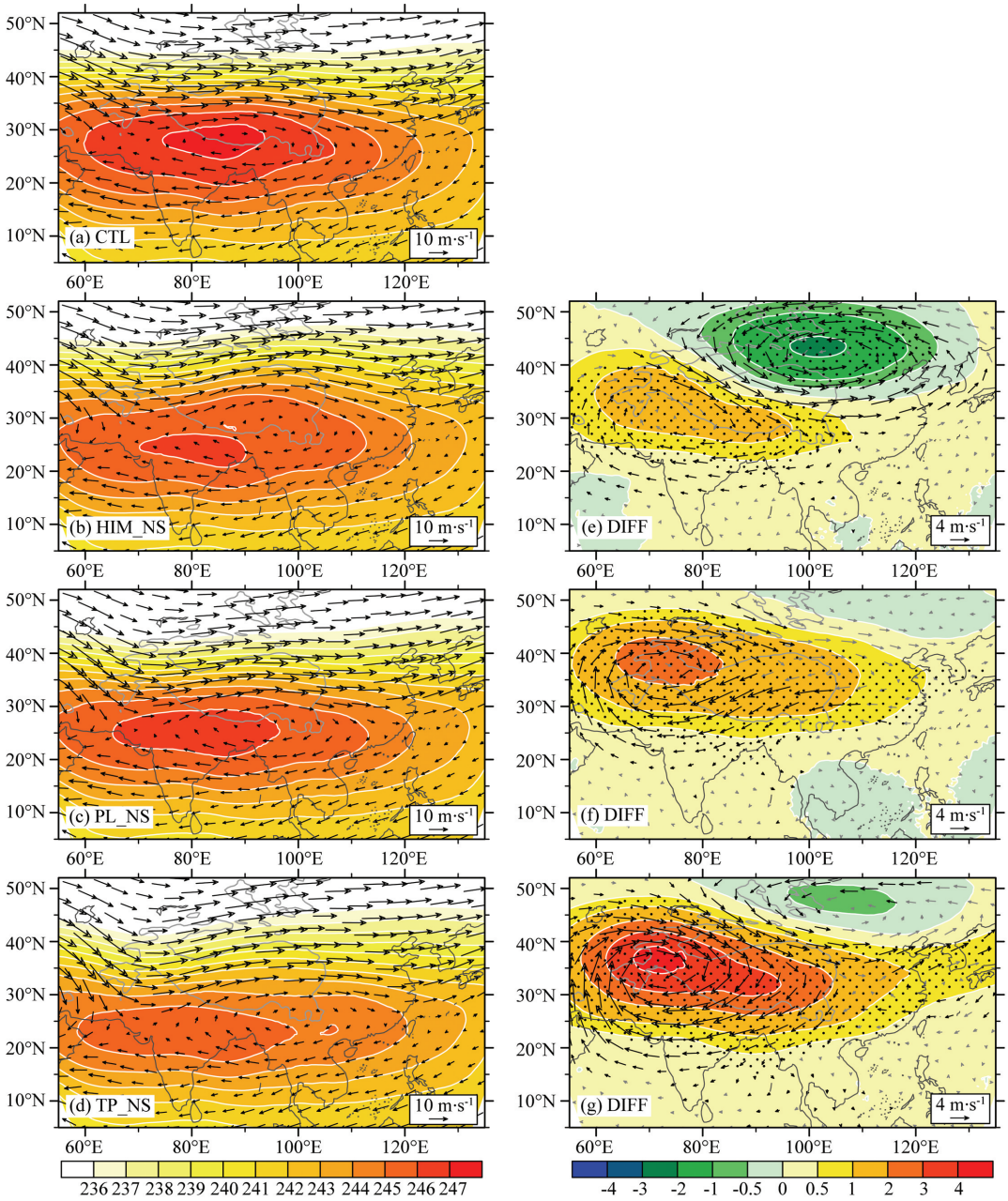

Fig. 6 Mass-weighted vertical mean temperature (shading, unit: K) and wind (vectors, unit: m·s^{-1}) for 400∼200 hPa in summer time

(a) CTL; (b) HIM_NS; (c) PL_NS; (d) TP_NS; (e) CTL minus HIM_NS; (f) CTL minus PL_NS, and (g) CTL minus TP_NS. Dotted regions in (e-g) denote the statistical significance of temperature anomalies above 95% level, and wind differences significant above 95% level are plotted in black color.

the SASM is intensified but resulted from the northward expansion of the southern branch. Actually, the northern branch of SASM disappeared at this time. If only the PL's heating is suppressed (Fig. 7c), both the southern and northern branch of SASM still exist. Almost all of the results in PL_NS are consistent with those in CTL, except for the weaker intensity of the ascending motion. It is noteworthy that thermal forcing over the HIM or PL can cause the local vertical circulation to be weak or disappear, but also make the ascending motion enhanced over the adverse area (where surface heating remains). Such as the ascending motion over the platform in HIM_NS (Fig. 7b) or the ascending motion over the TP's southern slope in PL_NS is stronger

than that in CTL experiment (Fig. 7a). It is not difficult to find that HIM's thermal forcing enhances local ascending motion over the southern slope but makes downward motion over the platform. While PL's heating effect contributes to upward motion over the platform but downward motion over the southern slope of TP. As a result, the upward motion will be partly offset if both the HIM's and PL's heatings exist (Fig. 7a), which is consistent with the results from the ideal orographic experiment with global climate model (Wang, 2005).

When the surface heating over the whole TP is removed, the northern branch of SASM is basically suppressed and the southern branch expands northward (similar to that in HIM_NS). And the upward motion over the northern slope also disappears in TP_NS, this is different from HIM_NS (Fig. 7b). On the other hand, it is relatively simplified for the vertical circulation of EASM. Both the HIM's and PL's heatings enhance the EASM vertical motion and benefit for the northward expansion of EASM (figure omitted).

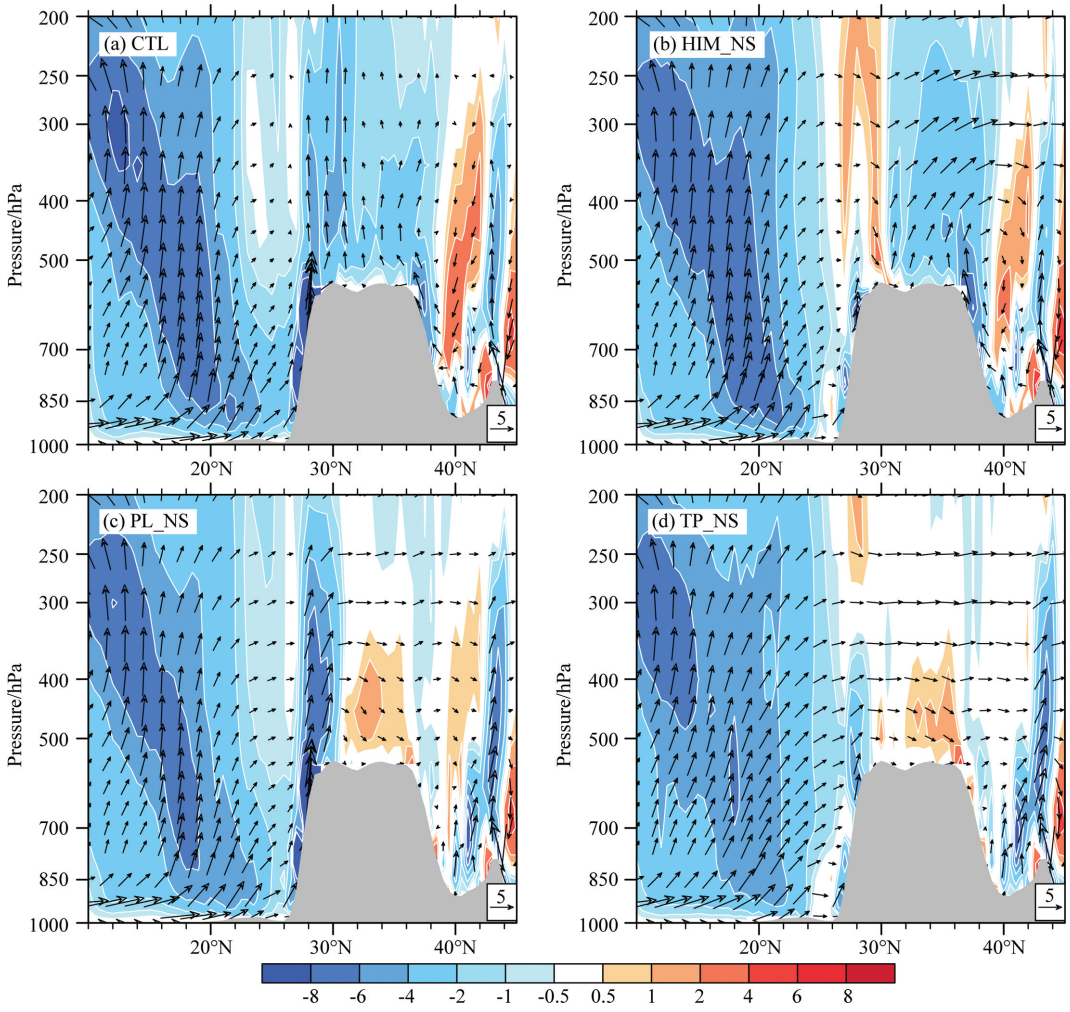

Fig. 7 Pressure-latitude cross-sections of the vertical circulation (vectors, v and $-50 \times \omega$, unit: 0.02 m·Pa·s^{-2}) and vertical velocity (shading, unit: 0.02 Pa·s^{-1}) averaged from 85°E to 90°E for the experiments (a) CTL; (b) HIM_NS; (c) PL_NS; (d) TP_NS.

3.3 Comparison of Different Monsoon Indices

To further clarify the different impacts of thermal forcing over different terrains of TP on ASM, Fig. 8 shows several commonly used monsoon indices. SA1 represents the difference of areal-averaged zonal wind between 850 hPa and 200 hPa over the south Asia region (5°N-20°N, 60°E-110°E) (Webster et al., 1998); SA2 is defined as the V850 minus V200 in Indian monsoon region and its eastern area (10°N-30°N, 70°E-110°E) (Goswami et al., 1999); SA3 is defined as areal-averaged U850 in South India (5°N-15°N, 60°E-80°E) minus areal-averaged

U850 in North India (20°N-30°N, 70°E-90°E) (Wang et al., 2001). The above mentioned monsoon indices represent different monsoon dynamics of the SASM, i.e. the overturning of monsoon zonal circulation (SA1), the meridional Hadley circulation (SA2), and the intensity of Indian monsoon trough (SA3). On the other hand, according to Wang et al. (2008b), EASM can be measured through the low-level southerly. EA1 is defined by the areal-averaged meridional wind at 850 hPa in East China (20°N-40°N, 110°E-120°E), which denotes the intensity of northward moisture transports. EA2 is defined as the difference between U850 in (20°N-30°N, 110°E-125°E) and U850 in (30°N-40°N, 110°E-125°E), representing the intensity of moisture convergence and its location over East Asia. The deviation of each index in each sensitive experiment from CTL can represent the effect intensity of thermal forcing over different terrain of the TP.

Figure 8 shows that both the SASM and EASM can be enhanced by TP's heating (the indices are decreased from CTL to TP_NS), except for Indian monsoon trough index (SA3). The largest amplitude occurs in TP_NS, and indices are not the same in the other two sensitive experiments, i.e. HIM_NS and PL_NS. Comparing monsoon indices in HIM_NS and PL_NS, we find that the HIM's sloping heating has a greater impact on the vertical zonal wind shear of SASM ($SA1_{HIM\_NS}<SA1_{PL\_NS}$); while the PL's heating has a stronger modulation on the meridional Hadley circulation ($SA2_{HIM\_NS}>SA2_{PL\_NS}$), corresponding with the result of previous analysis (thermal forcing over the PL influences the circulation on a larger spatial range). But why SA3 is amplified when the surface heating weakens? We can find some evidences in Figs. 4 and 5. Suppressed TP's heating weakens the northward climbing airflow from BOB but enhances the westward flow around the southern slope of TP, which lead to a stronger monsoon trough over northern India. Moreover, the enhanced amplitude of SA3 by HIM's heating is much stronger than the PL's heating. That is because the climbing airflow is basically suppressed after the sloping heating is removed in HIM_NS and absolutely turns into airflow around the southern TP (Fig. 5c). As to the EASM, HIM's heating not only enhances southerly over East China, but also contributes to northerly from high latitudes (Fig. 4f). The convergence of southerly and northerly makes EA1 smaller than that in CTL experiment. While there is no obvious response of abnormal northerly in the experiment of no PL's heating (Fig. 4g), thus the EA1 index in PL_NS has larger amplitude than that in HIM_NS. But to the EA2 index, indicating the intensity of moisture convergence over East China, the amplitude in HIM_NS is larger than that in PL_NS. Consequently, the abnormal precipitation is more significant in HIM_NS experiment (Fig. 4f).

From the above analyses, TP's orographic thermal forcing surely plays an important role in the formation and maintenance of ASM. Especially the Himalayas' sloping heating, it exerts a decisive impact on the formation of the northern branch of SASM. Furthermore, the comparison of multiple monsoon indices indicates that the surface heating over different terrain of the TP has a different influence on SASM and EASM, respectively.

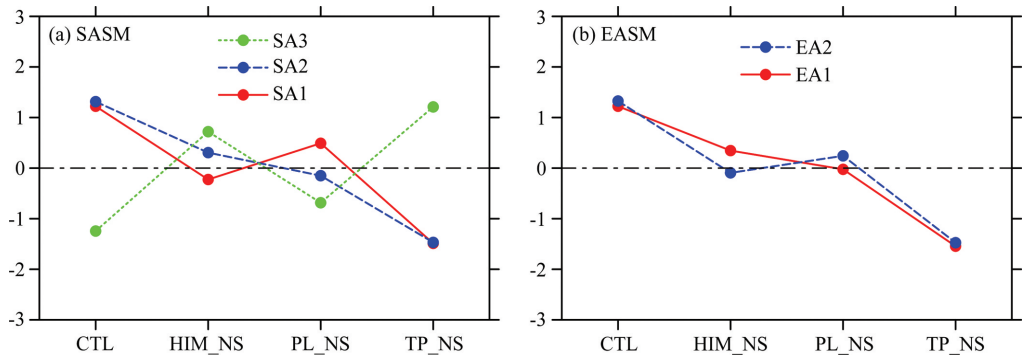

Fig. 8 Standardized monsoon indices in different experiments

(a) South Asian summer monsoon (SASM); (b) East Asian summer monsoon (EASM).

4 CONCLUSION AND DISCUSSION

Based on a high resolution regional model (WRF), the impact of thermal forcing over different terrains of the TP on the circulation, precipitation and temperature structure of SASM and EASM was investigated. The

main conclusions can be summarized as follows:

(1) The local circulation and precipitation around the HIM are significantly influenced by the surface heating over the TP's southern slope, which is a dominant factor for the formation of the north branch of SASM. Meanwhile, the climbing moist airflow and precipitation over the southern slope of the TP are mainly induced by HIM's thermal forcing. Due to HIM's sloping heating, the upper-level troposphere warm center is steadily located over the HIM area. HIM's heating also makes EASM intensified obviously, which is characterized both by the enhanced low-level southwesterly over East China and the enhanced southward anomalous dry-cold northerly.

(2) Although the influence of PL's heating on the summer monsoon circulation and precipitation is weaker than the HIM's, it induces a wider response of SASM and a stronger influence on the meridional Hadley circulation. The PL's heating is able to regulate low-level southwesterly over the remote tropical ocean. In addition, it also enhances the EASM.

(3) The ascending motion over the southern slope of TP disappears without the local HIM's heating, and meanwhile ascending motion over the TP's platform is enhanced. Otherwise, the absence of PL's heating suppresses the local ascending motion but enhances upward motion over the southern slope of TP.

(4) The comparison of multiple monsoon indices reveals that both HIM's sloping heating and PL's heating can intensify SASM or EASM, but the impacts of thermal forcing over different terrains are different on the two subsystems of ASM. For example, the HIM's sloping heating has a greater impact on the vertical zonal wind shear of SASM (SA1), while PL's heating has a stronger modulation on the meridional Hadley circulation (SA2). In addition, PL's heating has a more important effect on EA1 index, while HIM's heating regulates the moisture convergence (EA2) over East China more significantly.

Results in this study indicate that thermal forcing over the TP is the basic condition for local precipitation. Summer precipitation will disappear once TP's heating is suppressed. In other word, condensational latent heat associated with the precipitation is also reduced when the sensible heating is removed, weakening the whole heat source over the TP. Summer precipitation primarily occurs over the southern slope of TP, so the atmospheric heat source of TP weakens more significantly in the experiment of HIM_NS than that in PL_NS. This is the explanation for why the HIM's heating has a greater impact on climate than the PL's heating. It is worthy to discuss the effect of single condensational heating on the ASM in the future work. Furthermore, our results are based on regional atmospheric model and SST in this model is fixed with the observations, where air-sea interaction is absent. However, TP's heating certainly influences the sea surface wind (Fig. 4h), which may have a further impact on the SST. Of course, changed SST also exerts feedback to atmosphere, and then abnormal monsoon and precipitation will occur. Thus, how does the air-sea interaction modulate the relationship between the TP's heating and ASM? Is the effect of such modulation remarkable? The application of air-sea coupled model will give an answer to these questions in the future.

ACKNOWLEDGMENTS

The authors would like to thank Prof. Guoxiong Wu (Institute of Atmospheric Physics, Chinese Academy of Sciences) and the anonymous reviewers for their valuable comments and suggestions. This study was supported by the National Natural Science Foundation of Guangdong Province (2015A030310224), the National Key Research Program of China (2014CB953900), and the National Natural Science Foundation of China (91337216, 41605038).

References

Boos W R, Kuang Z M. 2010. Dominant control of the South Asian monsoon by orographic insulation versus plateau heating. *Nature*, 463(7278): 218-223.

Boos W R, Kuang Z M. 2013. Sensitivity of the South Asian monsoon to elevated and non-elevated heating. *Scientific Reports*, 3: 1192, doi: 10.1038/srep01192.

Flohn H. 1957. Large-scale aspects of the "summer monsoon" in South and East Asia. *Journal of the Meteorological Society of Japan*, 75: 180-186.

Goswami B N, Krishnamurthy V, Annmalai H. 1999. A broad-scale circulation index for the interannual variability of the Indian summer monsoon. *Quarterly Journal of Royal Meteorological Society*, 125(554): 611-633.

He B. 2012. Numerical simulation and mechanism study on the impacts of Tibetan Plateau thermodynamic forcing over South Asian summer monsoon [Ph. D. thesis] (in Chinese). Nanjing: Nanjing University of Information Science & Technology.

He J H, Xu H M, Zhong S S, et al. 2011. Characteristics of Atmospheric Heat Source over the Tibetan Plateau and Its Impacts and Possible Mechanisms (in Chinese). Beijing: China Meteorological Press.

Herring S C, Hoerling M P, Peterson T C, et al. 2014. Explaining extreme events of 2013 from a climate perspective. *Bulletin of the American Meteorological Society*, 95(9): S1-S104.

Kim E J, Hong S Y. 2010. Impact of air-sea interaction on East Asian summer monsoon climate in WRF. *Journal of Geophysical Research*, 115: D19118, doi: 10.1029/2009JD013253.

Li Y Q. 2003. Surface heating in the Tibetan Plateau and general circulation over it and their relations with the prediction of drought-flood at its eastern side. *Chinese Journal of Atmospheric Sciences* (in Chinese), 27(1): 107-114.

Liang X Y, Liu Y M, Wu G X. 2006. Roles of tropical and subtropical land-sea distribution and the Qinghai-Xizang Plateau in the formation of the Asian summer monsoon. *Chinese J. Geophys.* (in Chinese), 49(4): 983-992.

Mao J Y, Wu G X. 2006. Impacts of anomalies of thermal state over the Qinghai-Xizang Plateau and sea surface temperature on interannual variability of the Asian monsoon seasonal transition. *Chinese J. Geophys.* (in Chinese), 49(5): 1279-1287.

Molnar P, Boos W R, Battisti D S. 2010. Orographic controls on climate and paleoclimate of Asia: Thermal and mechanical roles for the Tibetan Plateau. *Annual Review of Earth and Planetary Sciences*, 38(1): 77-102.

Qian Y F, Yan H, Wang Q Q, et al. 1988. Numerical Study of the Effect of Topography in the Planetary Atmosphere (in Chinese). Beijing: Science Press, 105.

Skamarock W C, Klemp J B, Dudhia J, et al. 2008. A description of the advanced research WRF version 3. NCAR Technical Note NCAR/TN-475+STR, doi: 10.5065/D68S4MVH.

Wang B, Wu R G, Lau K M. 2001. Interannual variability of the Asian summer monsoon: contrasts between the Indian and the western North Pacific-East Asian monsoons. *Journal of Climate*, 14(20): 4073-4090.

Wang B, Bao Q, Hoskins B, et al. 2008a. Tibetan Plateau warming and precipitation changes in East Asia. *Geophysical Research Letters*, 35: L14702, doi: 10.1029/2008GL034330.

Wang B, Wu Z W, Li J P, et al. 2008b. How to measure the strength of the East Asian summer monsoon. *Journal of Climate*, 21(17): 4449-4463.

Wang Z Q, Duan A M, Wu G X. 2014a. Impacts of boundary layer parameterization schemes and air-sea coupling on WRF simulation of the East Asian summer monsoon. *Science China: Earth Science*, 57(7): 1480-1493, doi: 10.1007/s11430-013-4801-4.

Wang Z Q, Duan A M, Wu G X. 2014b. Time-lagged impact of spring sensible heat over the Tibetan Plateau on the summer rainfall anomaly in East China: case studies using the WRF model. *Climate Dynamics*, 42(11-12): 2885-2898, doi: 10.1007/s00382-013-1800-2.

Wang Z Q, Duan A M, Wu G X, et al. 2015. Mechanism for occurrence of precipitation over the southern slope of the Tibetan Plateau without local surface heating. *International Journal of Climatology*, doi: 10.1002/joc.4609.

Webster P J, Magaña V O, Palmer T N, et al. 1998. Monsoons: processes, predictability, and the prospects for prediction. *Journal of Geophysical Research*, 103(C7): 14451-14510.

Webster P J. 2006. The coupled monsoon system. // The Asian Monsoon. Berlin Heidelberg: Springer, 3-66.

Wu G X, Li W P, Guo H. 1997. Sensible heat driven air-pump over the Tibetan-Plateau and its impacts on the Asian Summer Monsoon. // Ye D Z ed. Collections on the Memory of Zhao Jiuzhang (in Chinese). Beijing: Science Press.

Wu G X, Zhang Y S. 1998. Tibetan Plateau forcing and the timing of the monsoon onset over South Asia and the South China Sea. *Monthly Weather Review*, 126: 913-927.

Wu G X, Liu Y M, Zhang Q, et al. 2007. The influence of mechanical and thermal forcing by the Tibetan Plateau on Asian climate. *Journal of Hydrometeorology*, 8(4): 770-789, doi: 10.1175/JHM609.1.

Wang Z Z. 2005. Numerical study of the Tibetan Plateau effects on weather and climate [Ph. D. thesis] (in Chinese). Beijing: Graduate University of Chinese Academy of Sciences.

Wu G X, Liu Y M, He B, et al. 2012. Thermal controls on the Asian Summer Monsoon. *Scientific Reports*, 2: 404, doi: 10.1038/srep00404.

Xu X D, Lu C G, Shi X H, et al. 2010. Large-scale topography of China: A factor for the seasonal progression of the Meiyu rainband? *Journal of Geophysical Research*, 115: D02110, doi: 10.1029/2009JD01244.

Yang H W, Wang B, Wang B. 2012. Reduction of systematic biases in regional climate downscaling through ensemble forcing. *Climate Dynamics*, 38(3-4): 655-665.

Ye D Z, Gao Y X, Zhou M Y, et al. 1979. Meteorology of the Qinghai-Xizang (Tibet) Plateau (in Chinese). Beijing: Science Press.

Yu E T, Wang H J, Gao Y Q, et al. 2011. Impacts of cumulus convective parameterization schemes on summer monsoon precipitation simulation over China. *Acta Meteorologica Sinica*, 25(5): 581-592.

Yu L J, Hu D X. 2008. Role of snow depth in spring of Tibetan Plateau in onset of South China Sea summer monsoon. *Chinese J. Geophys.* (in Chinese), 51(6): 1682-1694.

Zhang Y C, Qian Y F. 1999. Numerical studies on the effects of the critical height of Qinghai-Xizang Plateau uplift on the atmosphere. *Acta Meteorologica Sinica* (in Chinese), 57(2): 157-167.

Zhao P, Chen L X. 2001. Climatic features of atmospheric heat source/sink over the Qinghai-Xizang Plateau in 35 years and its relation to rainfall in China. *Science in China Series D: Earth Sciences*, 44(9): 858-864.